



## OPEN Retrograde evoked compound action potentials as an alternative for close-loop spinal cord stimulation

Nianshuang Wu<sup>1,2</sup>, Zhen Wu<sup>1,2</sup>, Cheng Zhang<sup>1,2</sup>, Changzhe Wu<sup>1</sup>, Xiaolin Huo<sup>1,2</sup>, Jinzhu Bai<sup>3,4</sup> & Guanghao Zhang<sup>1,2</sup>

Evoked compound action potential (ECAP) is an important parameter in close-loop spinal cord stimulation (SCS). The recording electrode is typically positioned proximal to the stimulation electrode to capture the antegrade ECAP signals generated by ascending fibers. However, relatively little research has been conducted on retrograde ECAPs. This study investigated retrograde ECAPs using custom-made epidural electrodes in 11 adult male Sprague–Dawley rats. Results show that the average motor threshold (MT) and ECAP threshold (ECAPT) for 11 anesthetized rats were  $218.18 \pm 69.54$   $\mu\text{A}$  and  $107.27 \pm 27.96$   $\mu\text{A}$ , respectively. The ECAP amplitudes increased with increase of the stimulation current and pulse width (PW), and were larger in awake rats than in anesthetized rats. Additionally, aside from ECAPs recorded by a commercial electrophysiological recorder, ECAPs were also recorded by a custom-made amplifier for the purpose of future long-term implantation, but the custom-made amplifier showed lower signal to noise ratio than the commercial amplifier. In conclusion, this study illustrates that retrograde ECAP may also be considered as a feedback signal for close-loop SCS and more sophisticated ECAP recording circuits are needed to form a close-loop system.

**Keywords** Spinal cord stimulation, Evoked compound action potential, Close-loop, Motor threshold

Spinal cord stimulation (SCS), as a safe and effective neuromodulation method, has been used to treat various types of chronic pain, especially refractory chronic pain<sup>1,2</sup>. The "gate control theory" proposed by Melzack and Wall in 1965 suggests that there is a pathway in the spinal cord that controls the transmission of pain signals to the brain<sup>3</sup>. The SCS induced activation of large-diameter A $\beta$  fibers, which do not conduct nociceptive signals, inhibits the transmission of pain signals from small-diameter A $\delta$  and C fibers through inhibitory interneurons, thereby achieving an analgesic effect<sup>4</sup>.

SCS electrodes are usually inserted into the spinal canal in the lumbar section of the spine and extending to the T7–T10 segments, adjusted according to the range of pain. Clinically significant epidural lead migration occurs in the early SCS trial period and after SCS implant<sup>5–8</sup>. The rate of lead migration in patients who have received spinal cord stimulator implants is approximately one in ten patients<sup>9</sup>. Slight migration of the lead may result in a shift of the activating field and loss of the desired paresthesia<sup>10</sup>. Furthermore, the shifting of the spinal cord within the subarachnoid space as the body position changes alters the distance between the electrode and the targeted stimulation area. This variation can lead to either inadequate or excessive stimulation intensity for SCS, which often results in discomfort for most patients during positional changes. In order to adjust the stimulus strength, patients need to remotely control the amplitude of the stimulus to reduce the possibility of excessive stimulation, while also minimizing the extent of the painful area<sup>11</sup>. In response to the challenges posed by positional changes, a cutting-edge close-loop SCS system utilizing accelerometers has come to the forefront. This innovative system is capable of sensing alterations in the electrode's position and dynamically adjusting the output current amplitude to maintain optimal stimulation levels. Clinical experimental results showed that 80.3% of patients experienced increased comfort during position changes<sup>12</sup>. The therapeutic benefits of SCS are realized through the activation of spinal sensory fibers. However, the output of close-loop stimulation systems

<sup>1</sup>Beijing Key Laboratory of Bioelectromagnetism, Institute of Electrical Engineering, Chinese Academy of Sciences, Beijing 100190, China. <sup>2</sup>School of Electronic, Electrical and Communication Engineering, University of Chinese Academy of Sciences, Beijing 100049, China. <sup>3</sup>Department of Spine and Spinal Cord Surgery, Beijing Bo'ai Hospital, Rehabilitation Research Center, Beijing, China. <sup>4</sup>School of Rehabilitation Medicine, Capital Medical University, Beijing, China. ✉email: zhangguanghao@mail.iee.ac.cn

that rely on accelerometers currently lacks the capability to adjust in real-time based on the excitability of these sensory fibers. To address these issues, it is possible to conduct real-time in vivo recordings of evoked compound action potentials (ECAPs) during SCS, which allows for a more precise adjustment of the stimulus strength<sup>13,14</sup>. The spinal ECAP recorded in clinical trials has a triphasic shape, including a positive peak (P1), followed by a sharp negative peak (N1), and ending with a second positive peak (P2), with a conduction velocity between 37 and 82 m/s<sup>15–17</sup>. For each stimulus pulse delivered, ECAPs can delineate the range of sensory fiber activation, thereby enabling an estimation of the pain coverage area achieved by SCS. In a close-loop SCS system based on ECAP, the stimulation current is automatically modulated to minimize discrepancies between the measured ECAP and the desired target ECAP. This adjustment aims to stabilize the activation level of sensory fibers within the spinal cord's target area, thereby maximizing the therapeutic efficacy of the treatment. Clinical trial outcomes demonstrated that a greater proportion of patients in the ECAP close-loop SCS group achieved therapeutic success, defined as a reduction in pain of more than 50%, when compared to the open-loop SCS group<sup>18–22</sup>. Substantial research has been dedicated to antegrade ECAPs, as they are intimately connected to the excitation state of the dorsal column sensory fibers. However, in cases where stimulation contacts must be adjusted to the two most rostral channels following permanent electrode implantation, there are no contacts available for capturing antegrade ECAPs, whereas contacts located on the caudal portion of the electrode lead can only record retrograde ECAPs. In instances of spinal cord injuries, SCS leads are typically implanted at segments of the spine caudal to the injury plane, such as L1-S1<sup>23</sup>, L1-T11<sup>24</sup> or L4-L1<sup>25</sup>. These placements aim to activate descending motor fibers, thereby facilitating the restoration of walking function. In such scenarios, descending ECAPs have proven to offer more reliable feedback compared to ascending ECAPs. Consequently, it becomes imperative to explore alternative indicators, such as retrograde ECAPs, to furnish supplementary feedback for effective pain management.

ECAPs captured in animal studies, being more accessible, offer valuable insights into the fundamental properties of ECAPs. In sheep experiments, ECAPs elicited by electrical stimulation were recorded using epidural SCS leads that were implanted within the spinal canal. These ECAPs presented a triphasic waveform, with their amplitude and dispersion being intricately linked to the diameter and location of the fibers<sup>14,26,27</sup>. In rat experiments, a second lead was placed subcutaneously to serve as the ground electrode to ensure stable and high-quality signal acquisition<sup>28</sup>, which is not feasible in clinical trials. ECAPs from the rat spinal cord consistently displayed the anticipated triphasic morphology under both anesthetized and conscious conditions<sup>28</sup>. Implementing ECAP-based SCS parameters within a close-loop SCS system has been shown to effectively induce analgesia in animals in experimental models of neuropathic pain<sup>29</sup>. Therefore, we can optimize the parameters of close-loop SCS in animal experiments to provide reference for future clinical applications.

In this study, we hypothesized that retrograde ECAPs are as efficient and stable as antegrade ECAP for close-loop SCS. A custom-made epidural electrode was rostrally inserted into the spinal canal of rats to stimulate the T1–T3 section of the spinal cord and record the retrograde ECAP at the T10–T12 section. The ECAPs induced by different stimulation currents and pulse widths (PWs) were recorded to find the motor threshold (MT) and ECAP threshold (ECAPT). ECAP responses were compared between anesthetized and awake states. A custom-made amplifier based on the AD620 was used to investigate the measurement parameters for future fully implanted close-loop stimulator. The findings in this study may provide a basis for improving close-loop SCS systems with both antegrade and retrograde ECAP.

## Results

### MTs and ECAPTs under anesthesia

When using a floating ground in commercial amplifier, the recorded ECAP signal was overwhelmed by loud noise. Signals recorded using the other three grounding methods showed relatively small noise. Using channel 4 on the implanted lead as the ground also showed a peak-to-peak noise level of 100  $\mu$ V. Therefore, we used channel 4 as ground in the following experiments.

With a stimulation PW of 200  $\mu$ s, the MTs and ECAPTs for the 11 rats in the anesthetized state are illustrated in Fig. 1. As shown in Fig. 1a, the MT is always larger than ECAPT in the same rat and the MT is at least 1.25 times that of ECAPT. The maximum and minimum MTs were 310  $\mu$ A and 110  $\mu$ A, respectively, while the maximum and minimum ECAPTs were 140  $\mu$ A and 70  $\mu$ A, respectively. T-test result show that the MT ( $218.18 \pm 69.54$   $\mu$ A) is larger than ECAPT ( $107.27 \pm 27.96$   $\mu$ A) ( $p < 0.001$ ). The MTs have a larger coefficient of variance (CV) of 31.87%, whereas the ECAPT have a relatively small CV of 26.07% ( $F = 6.19$ ,  $p = 0.004$ ) as shown in Fig. 1b. By clarifying the relationship between MT and ECAPT, the future close-loop SCS system may automatically set an initial stimulation current between MT and ECAPT, as well as an appropriate step size range, reducing the time needed for clinicians to manually adjust parameters and improving clinical efficiency.

### ECAP responses under different stimulation currents and PWs

Figure 2 illustrates the ECAP responses of Rat 2 under different stimulation currents and PWs. The MT and ECAPT of this rat were 260  $\mu$ A and 140  $\mu$ A respectively. The ECAP caused by each stimulation current and PW shows similar dynamic process within 0 to 3 ms, characterized by two positive peaks and one negative peak. The spinal ECAP elicited by different stimulation current are shown in Fig. 2a. The P1, N1 and P2 peaks observed in the measurements are labeled in the legends. No ECAP was observed at a stimulation current of 100  $\mu$ A. As the stimulation current increased from 140 to 400  $\mu$ A, the ECAP amplitude increased from 0.16 to 0.63 mV. When the stimulation current increased from 260 to 400  $\mu$ A, the intensity of muscle twitching also increased, while no muscle twitching was observed when the stimulation current was less than 260  $\mu$ A. We noticed the ECAP amplitude nearly saturated when the stimulation current exceeded 260  $\mu$ A. This phenomenon typically occurs when all nerve fibers, including the nerve roots, have been fully activated. Further increases in stimulation current do not result in additional fiber activation. The changes in ECAP response under different stimulation

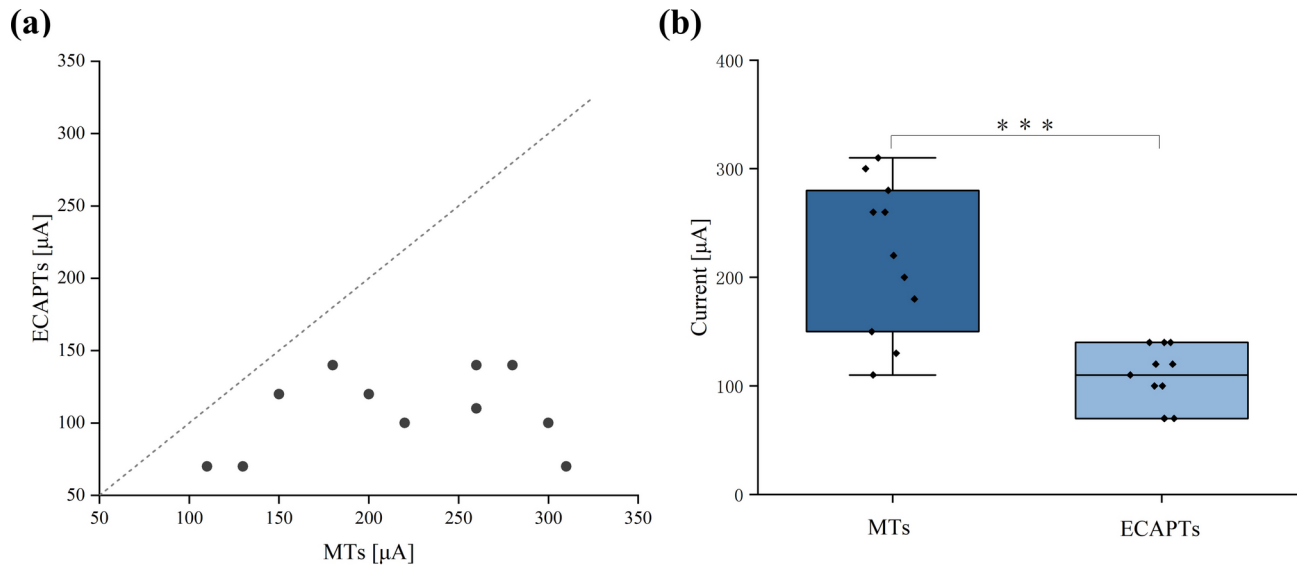


**Fig. 1.** MTs and ECAPTs for 11 rats in the anesthetized state. **(a)** The distribution of MTs and ECAPTs for 11 rats. **(b)** MTs are larger than ECAPTs.

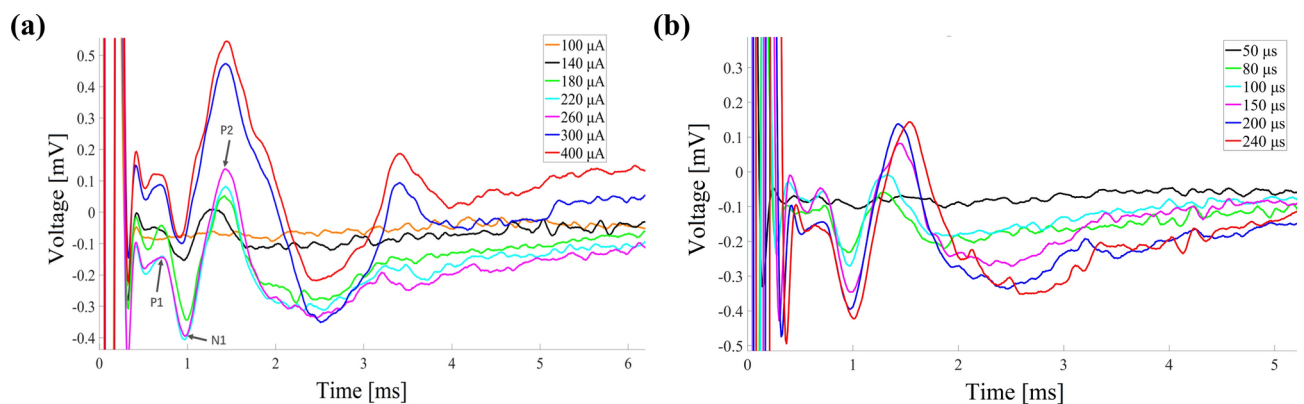


**Fig. 2.** ECAP response under different stimulation currents and PWs. **(a)** The ECAP responses with a PW of 200 μs and stimulation currents ranging from 100 to 400 μA. **(b)** The ECAP responses with a stimulation current of 260 μA and PWs ranging from 50 to 240 μs.

PWs, ranging from 50 to 240 μs, are shown in Fig. 2b. No ECAP was observed at a stimulation PW of 50 μs. As the stimulation PW increased from 80 to 240 μs, the ECAP amplitude correspondingly increased from 0.17 to 0.57 mV. At a stimulation pulse width of 240 μs, muscle twitching was also more pronounced, whereas no muscle twitching was observed when the stimulation pulse width was less than 200 μs. The remaining 10 rats exhibited similar results.

#### Comparison of the ECAP amplitudes between the anesthetized and awake states

The differences in ECAP responses between anesthetized and awake states under the same stimulation parameters (stimulation current = 140 μA, PW = 200 μs) are illustrated in Fig. 3. T-test result revealed the ECAP amplitude in the anesthetized state ( $0.23 \pm 0.092$  mV) was less than the ECAP amplitude in the awake state ( $0.40 \pm 0.29$  mV) ( $p < 0.05$ ). We suppose that the suppression of neural excitability may lead to lower ECAP amplitudes during anesthesia, and therefore lower ECAP thresholds may be required in the awake state to achieve optimal stimulation effects.

#### ECAP waveforms were collected using the AD620

ECAP waveforms recorded by different acquisition systems are shown in Fig. 4, using Rat 11 as an example. The MT and ECAPT of this rat, recorded by MP150, are 110 μA and 70 μA respectively. Figure 4a shows the ECAPs recorded by AD620 when the stimulation currents varied from 100 to 500 μA and the PW remained 200 μs. No ECAP was observed under stimulation currents of 100–200 μA with the AD620. With the AD620, ECAPs with a triphasic structure were only observed when the stimulation current exceeded 300 μA. But we observed a clear

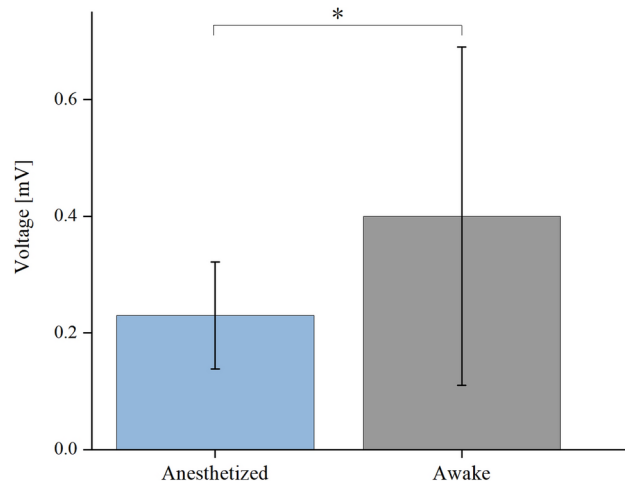


**Fig. 3.** Comparison of ECAP amplitudes caused by the same current and PW in 11 rats under anesthetized and awake conditions.

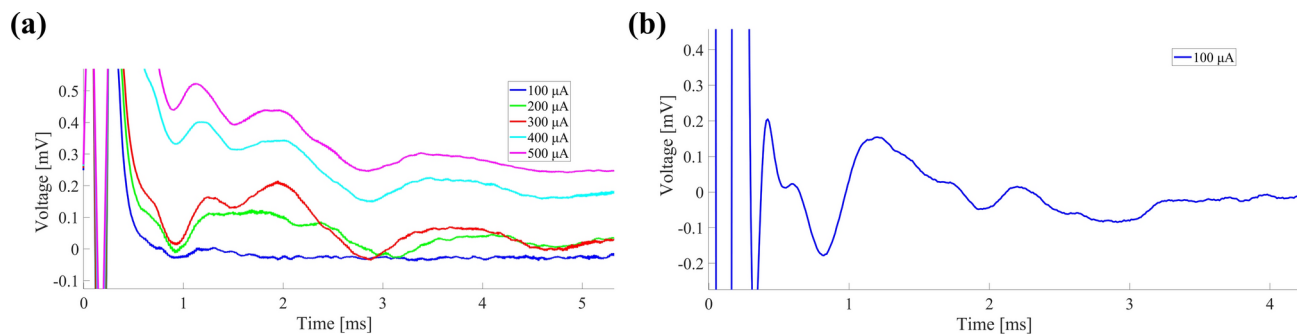


**Fig. 4.** ECAP waveforms recorded by two acquisition systems. (a) ECAPs recorded by the AD620. (b) ECAP recorded by MP150.

ECAP waveform recorded by MP150 when a stimulation current of 100  $\mu\text{A}$  was applied. The remaining 10 rats exhibited similar results. These results revealed that the signal collected by AD620 has poorer quality compared with MP150, and it is still necessary to add filtering circuits to improve signal quality.

## Discussion

Currently, the close-loop SCS systems that using ascending or antegrade ECAPs as feedback signals have been used in clinical trials and results have shown that they are more effective than traditional open-loop systems. Descending ECAPs were used in diagnosing the integrity of neural pathway of reconstruction of walking after paralysis caused by spinal cord injury. In this study, our main innovation lies in extending the use of descending or retrograde ECAPs to the close-loop SCS system as a substitute and/or supplement feedback parameter to improve the management of refractory pain. Our study also provides preliminary measuring circuitry for close-loop stimulators using retrograde ECAP. Our findings may offer a new approach to improve the current close-loop SCS strategy and optimize the personalized parameter adjustment process in long-term chronic pain management, thereby further improving treatment outcomes and patient comfort.

Lead migration is a common challenge for SCS systems during long-term use, especially for patients who wish to live independently. They often experience various body position changes such as sitting, lying down, standing, squatting, and bending over in daily life. Changes in body position can cause lead migration, which may result in a shift of the activation field and loss of the desired paresthesia. Existing literature has reported that close-loop SCS based on antegrade ECAP significantly improves clinical outcomes compared to open-loop systems. Specifically, when migration occurs in the ventral-dorsal direction, delivering stimulation current at the rostral and caudal contacts separately may lead to overstimulation on one side and insufficient stimulation on the other, corresponding to a larger retrograde ECAP and a small antegrade ECAP and vice versa. Lateral migration of electrodes can result in insufficient stimulation at both rostral and caudal ends, corresponding to small amplitudes of both antegrade and retrograde ECAPs. In such cases, retrograde ECAPs provide additional feedback signals, enabling the system to better detect changes in electrode position and promptly adjust stimulation parameters, preventing imbalanced stimulation caused by migration. We believe that simultaneously using both antegrade and retrograde ECAPs as feedback signals may help detect and compensate for lead migration, thereby achieving

more precise stimulation control and optimizing long-term outcomes for patients. However, retrograde ECAPs would not be more stable or less affected by physiological or anatomical variations than antegrade ECAPs. The antegrade ECAP is still the first choice in close-loop SCS. The retrograde ECAPs could serve as a substitute and/or supplement to antegrade ECAPs.

In our study, there are significant differences between the retrograde MTs and ECAPTs in the 11 rats under anesthesia. The average ECAPT was  $107.27 \pm 27.96 \mu\text{A}$ , which was similar to the antegrade ECAPT of  $130 \pm 20 \mu\text{A}$  in a previous study<sup>28</sup>. However, the average MT was  $218.18 \pm 69.54 \mu\text{A}$ , which was about 1/5 of the value in the previous study<sup>17</sup>. Different from previous studies, our study focuses on recording retrograde ECAPs using the same electrode that also delivers stimulation currents. The electrode location in sheep model significantly affected ECAP amplitude, with the highest amplitudes recorded in the midvertebral position and the lowest in the intervertebral disc regions<sup>14</sup>. Sharma et al. used a multimodal approach, employing separate electrodes for stimulating and recording descending electrophysiological signals<sup>30</sup>, while Deshmukh et al. focused on optimizing the recording techniques for ascending ECAPs during SCS<sup>31</sup>. Moreover, we noticed the CV of MT is larger than ECAPT ( $F=6.19, p=0.004$ ). MT corresponds to the activation threshold of the descending fibers and nerve roots further from the stimulation electrode. Slight lead migration may cause larger positional errors for electrodes targeting descending fibers or nerve roots than for those targeting the dorsal column, and thereby result in a larger CV for MT.

The amplitudes of ECAP increased as the stimulation current increased from 140 to 260  $\mu\text{A}$  in this study, because higher stimulation currents activate more fibers and result in stronger neural responses. This result is consistent with previous findings regarding antegrade ECAP, indicating that ECAP amplitude can be regarded as a feedback parameter to control stimulation current. However, the amplitudes of ECAP showed a phenomenon of saturation when stimulation currents exceeded MT. These saturation points or MT may be used as one factor to set a safety threshold in clinical applications. But the safety threshold needs to fully account for the risks of overstimulation and potential nerve damage, not just the activation of nerve fibers. During the process of acquiring MT, we observed that small muscle twitches caused by SCS often occurred near the surgical incision. The motor tract of the spinal cord in rats, specifically the corticospinal tract (CST), which controls motor function, is located in the ventral and lateral funiculi of the spinal cord, relatively near the midline on the ventral (anterior) side, not the dorsal (posterior) side. We speculate that electrical stimulation at T1-T3 spinal segments in this study activated a part of the spinal nerve root, thus causing muscle twitches in both the body and hindlimbs. While the clinical SCS electrodes are often implanted through lumbar puncture from bottom to top<sup>32</sup>, stimulation current larger than MT may also cause muscle twitched. This result illustrates that the stimulation current should be adjusted in a narrower range in close-loop SCS to avoid overstimulation.

We investigated the relationship between stimulation PW and ECAP amplitude. Longer PWs can more effectively stimulate nerve fibers and enhance neuronal excitability. Previous studies have demonstrated that the threshold for the generation of an action potential typically follows the shape  $f(x) = 1/x$ , known as the “strength-duration curve”, where the product of amplitude and PW (i.e., the charge per pulse) is constant across all points on the curve<sup>33</sup>. Our results are consistent with the conclusions of these references. However, the selection of stimulus PW must ensure that it does not affect the ECAP waveform; that is, the PW should be less than the ECAP latency, which is no less than 1 ms in this study.

The significant difference in ECAP amplitudes between anesthetized ( $0.23 \pm 0.092 \text{ mV}$ ) and awake states ( $0.40 \pm 0.29 \text{ mV}$ ) underscores the impact of anesthetic drugs on ECAP responses. This result suggests that smaller ECAPT and MT should be used in awake state to achieve close-loop stimulation. We suppose that the smaller amplitudes of ECAP in anesthetized state were mainly caused by the reduced excitability of the nervous system, resulting in fewer activated fibers. Anesthetics do indeed suppress neural activity, but there is currently no conclusive evidence indicating a significant difference in human ECAPs between anesthetized and awake states. This is an issue that we believe requires further research to clarify. Additionally, it should be noted that SCS surgeries are typically performed under local anesthesia, whereas our animal experiments were conducted under general anesthesia with ventilator assistance, which could lead to differences in neural excitability. Although our rat experiments showed a significant effect of anesthesia on ECAPs, it is not yet clear whether this conclusion applies to clinical human patients. Considering the suppressive effect that anesthesia may have on neural excitability, it may be necessary to adjust stimulation parameters post-operatively to accommodate the patient's nervous system once they are awake. Such adjustments aim to avoid both overstimulation and understimulation, ensuring effective pain management while preventing discomfort. This is an important clinical issue, and future research will focus on gaining a deeper understanding of the specific effects of anesthesia on ECAPs and the efficacy of SCS.

The design of the ECAP acquisition circuit directly affects the signal-to-noise ratio of the ECAP signal and the accuracy of close-loop control. We used a self-made AD620 module to record the ECAP with the positive and negative input terminals connected to channels 5 and 6 of the electrodes. The results indicate that when the ground channel is suspended, the signal noise significantly increases, while the signal-to-noise ratios of the other three grounding methods are all relatively low. Therefore, we suggest use the shell of the implanted pulse generator as the ground in future clinical trials, allowing more channels to be used for selective stimulation. However, the ECAP amplitudes recorded by the AD620 module were much smaller than those recorded by the MP150. This result suggests that the signal-to-noise ratio and other performance aspects of the AD620 module require further improvement, especially for later fully implanted animal experiments to ensure clear neural signal acquisition in the complex in vivo environment. In the future, we will improve the performance of the self-made recording system by increasing the input impedance, adjusting the gain of the amplifier, optimizing filters, and adding noise-reducing components, as well as reducing the size of the circuit. With these improvements, we will design a long-term implantable close-loop stimulator for sheep experiments, using both antegrade and



retrograde ECAPs as feedback signals. We will also consider using sheep as a pain model to investigate the effect of close-loop SCS.

## Conclusion

This study conducted a detailed analysis of the retrograde spinal ECAP response in rats under anesthetized and awake states, revealing the characteristics of ECAP under different stimulation currents and PWs. Retrograde ECAP may also be considered as a feedback signal for close-loop SCS. An ECAP recording circuit more sophisticated than the basic amplifier like the AD620 is needed to form a close-loop system. This study may provide a basis for improving close-loop SCS systems.

## Methods

### Subjects

Adult male Sprague–Dawley rats ( $n = 11$ ; 8–10 weeks old; 200–250 g; from Huaafukang, Inc., China) were used in this study. Upon arrival, the rats were allowed to acclimate for at least seven days in the Animal Laboratory of the China Rehabilitation Research Center before any experimental procedures were conducted. The rats were housed in groups of five per cage under a regular 12-h light/dark cycle (lights on at 8:00 a.m. and off at 8:00 p.m.), with temperature maintained at 21 °C and humidity at 55%. They had free access to standard laboratory rodent chow and water. To ensure familiarity with the testing procedures, the animals were habituated for at least three to four days prior to the experiments. All handling and testing were performed during the light phase (between 9:00 a.m. and 4:00 p.m.). Efforts were made to minimize animal suffering and to use the fewest number of animals possible. All surgical procedures were conducted according to the National Guidelines for Experimental Animal Welfare. And all study participants adhered to the ARRIVE guidelines. This study was approved by the Animal Experiments and Experimental Animal Welfare Committee of Capital Medical University (approval No. AEEI-2021-204) on July 26, 2021.

### Study design

A custom-made epidural lead (New Cloud Medical, Inc., China) features a flexible polyethylene printed circuit design, measuring 61.85 mm in length and 1.25 mm in width. As illustrated in Fig. 5, it consists of eight exposed stimulation channels, each measuring 0.3 mm  $\times$  1 mm. These channels are equally spaced at 4 mm intervals, connected to individual recording channels, and insulated on one side. Prior to implantation, the lead was disinfected with 75% ethyl alcohol. All rats underwent epidural lead implantation under general anesthesia using a compact small animal anesthesia machine (model TAI-IE, RWD, China) with air as the carrier gas. Initially, the rats were placed in the induction chamber with an oxygen flow rate of 1 L/min and an isoflurane concentration of 3.5%. After anesthesia was achieved, the rats were transferred to the surgical table and maintained with a nose cone delivering 0.6 L/min oxygen flow and 2.5% isoflurane concentration.

Typically, SCS electrodes span 3–4 spinal segments in human patients. However, given the shorter spinal cord length in rats, the range for stimulation and recording has been optimized to its maximum extent. Shortening the distance between electrode contacts brings great difficulties to the manufacturing process, and the amplitude of ECAP signals will also decrease, causing certain difficulties in signal acquisition. A small laminectomy was performed at the T11 (or T10 or T12) vertebral level, and the lead was inserted rostrally into the epidural space, with the tip of the electrode spanning the spinal levels between T1–T3 corresponding to the thoracic region, because the T10 segment of the thoracic vertebrae in rats can be located by touching the back to find the highest point of the thoracic vertebrae. T1–T3 segments are selected to avoid interference from stimulation signals during recording, it is advisable to separate the recording and stimulating electrodes as far as possible to ensure that the stimulation signals can be separated from the ECAPs. The lead was fixed in place with suture to the

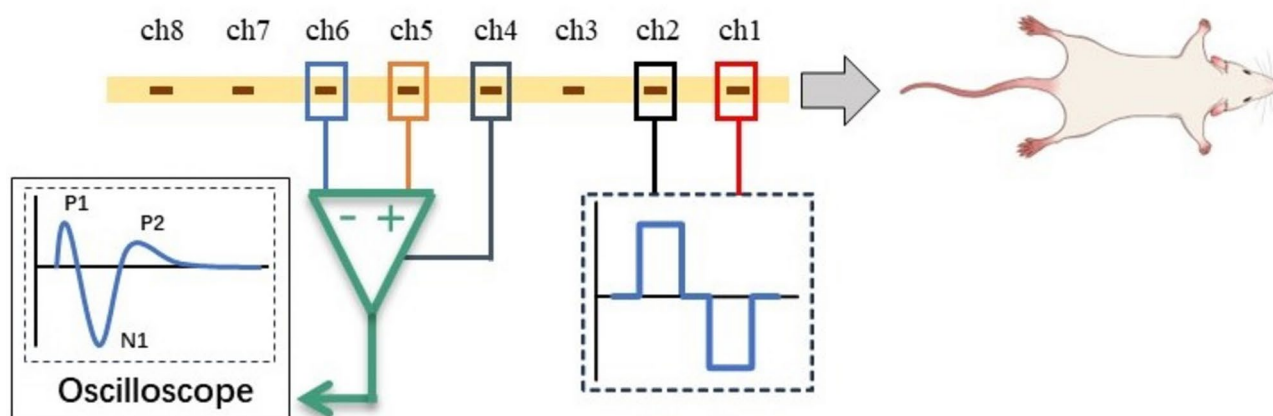


**Fig. 5.** The schematic diagram of the experiment procedure. The electrode has 8 channels, with ch1 and ch2 used for stimulation. The stimulation current is a biphasic square wave with a frequency of 0.5 Hz. Ch5 and ch6 are connected to an oscilloscope to collect ECAP signals, and ch4 is grounded.

muscle, the wound was sutured in layers, and the distal end of the lead was tunneled subcutaneously to exit the skin at the base of the tail for later ECAP recordings. The experimental design and recording setup are illustrated in Fig. 5. After recording ECAPs and MTs in both anesthetized and awake states, the experiment was terminated.

### Electrophysiology

Evoked responses were recorded and stored using the MP150 biomedical engineering signal recording and analysis system (Biopac, Inc., USA). Channels 5 and 6 were connected to Vin+ and Vin− on MP150, respectively. Channels 1 and 2 of the leads were connected to a cable that provided stimulation via a stimulator (3 Brain, Inc., USA). We first tested the influence of ground selections on the recorded ECAP in rat 1 using a current of 500  $\mu$ A, with a PW of 200  $\mu$ s. A needle electrode was inserted into different locations of the rat, including the tail, muscle near the incision and spinal cord, as well as a floating ground. The location of ground with the smallest noise was then used in the following experiments. A stepwise increase in stimulation current was employed to determine the depolarization threshold required to generate ECAPs. The stimulation current was gradually increased from 0  $\mu$ A until ECAP responses were observed on the MP150, with a stimulation frequency of 0.5 Hz and a biphasic PW of 200  $\mu$ s. ECAPT was defined as the stimulation current necessary to elicit an observable ECAP signal. The current was further increased until motor twitch was visually observed. MT was defined as the stimulation current required to induce a slight muscle contraction in the mid-lower trunk or hind leg, as visually observed by the experimenter. All MTs were recorded manually during experiments. Due to individual differences among the experimental rats, the step size of the current varied. To determine the shape of ECAPs and further characterize their relationship with previous studies in humans and sheep, the depolarization threshold for ECAPs was maintained while the PW was gradually reduced until ECAP responses were no longer visible. The ECAP amplitude, defined as the difference between the N1 and P2 peaks of each ECAP waveform, was calculated to compare the responses of rats under different stimulation parameters.

### Measurement circuit design

The commercial recording system we utilized was not intended for full implantation, which introduced a significant constraint in the development of our close-loop SCS system. To overcome this limitation, we opted to design and implement a specialized amplifier. The AD620 module, recognized for its cost-effectiveness and frequent application, was deemed appropriate for our needs. We employed the AD620 module to capture ECAPs, adhering to the measurement protocols outlined earlier using the MP150 system. The custom-made recording circuit is depicted in Fig. 6. The core chip AD620 was powered by  $\pm 5$  V battery-based voltage source. The gain of the amplifier was tuned to 2000 by adjusting the variable resistor connected to pin 1 and pin 8. Channels 5 and 6 of the lead were connected to the positive and negative input terminals (+IN and −IN) of the AD620, respectively. The output of the AD620 was connected to an oscilloscope (PicoScope 6402D, Pico Technology Co., England), where the signal was saved for further processing and analysis.

### Data processing

Data processing was conducted through the following steps. First, the 50 Hz power line interference in raw signals were filtered using a band-stop IIR filter within the Acknowledge software integrated into the MP150 system. ECAPTs were then manually collected by extracting the observed ECAP signals from the filtered waveforms. For each rat, the ECAPT and MT were calculated by averaging the values across two to six stimulation trials, as they varied between individual rats. Subsequently, the P1, N1 and P2 peaks were computed and analyzed using custom MATLAB scripts (2013 release, MathWorks Inc., Natick, MA). T-test was employed to statistically analyze the MTs and ECAPTs of rats under anesthesia, as well as the ECAP amplitudes in both anesthetized and

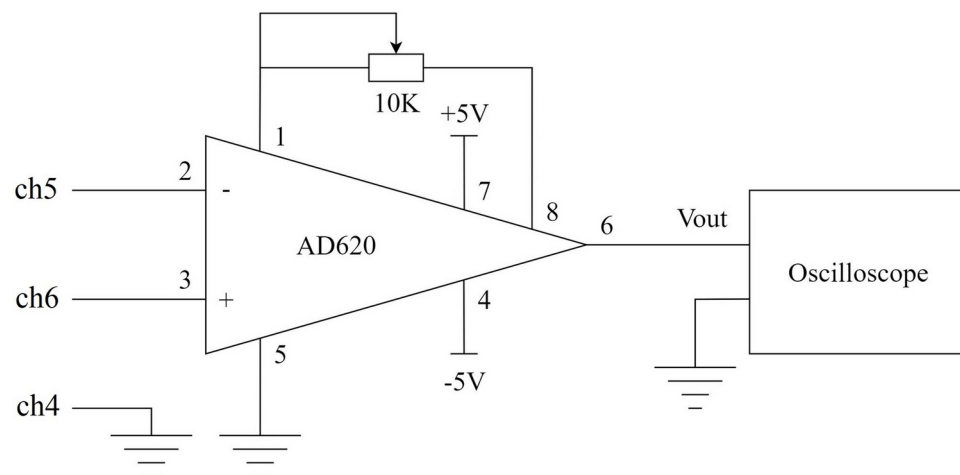


**Fig. 6.** The schematic diagram of the AD620 and oscilloscope connection. This setup is designed to amplify the ECAP signals recorded by the electrode channels (ch5 and ch6) and display them on the oscilloscope for further analysis. Ch4 serves as the ground to ensure the stability and accuracy of signal acquisition.

awake states. F-test was used to compare the CV of MTs and ECAPTs under anesthesia. Statistical analysis was performed using IBM SPSS Statistics V.26.0 (SPSS), with a significance level set at  $p < 0.05$ .

## Data availability

The datasets used or analyzed during the current study are available from the corresponding author on reasonable request.

Received: 8 July 2024; Accepted: 28 November 2024

Published online: 03 December 2024

## References

- Falowski, S., Celii, A. & Sharan, A. Spinal cord stimulation: an update. *Neurotherapeutics* **5**, 86–99. <https://doi.org/10.1016/j.nurt.2007.10.066> (2008).
- Deer, T. R. et al. The appropriate use of neurostimulation of the spinal cord and peripheral nervous system for the treatment of chronic pain and ischemic diseases: the Neuromodulation Appropriateness Consensus Committee. *Neuromodulation* **17**, 515–550. <https://doi.org/10.1111/ner.12208> (2014) (discussion 550).
- Melzack, R. & Wall, P. D. Pain mechanisms: a new theory. *Science* **150**, 971–979. <https://doi.org/10.1126/science.150.3699.971> (1965).
- Ong Sio, L. C., Hom, B., Garg, S. & Abd-Elsayed, A. Mechanism of action of peripheral nerve stimulation for chronic pain: a narrative review. *Int. J. Mol. Sci.* <https://doi.org/10.3390/ijms24054540> (2023).
- Song, W. H. C., Jen, T. T. H., Osborn, J. A. & Varshney, V. Early epidural lead migration in spinal cord stimulator trials: A case series. *Interv. Pain Med.* **3**, 100426. <https://doi.org/10.1016/j.inpm.2024.100426> (2024).
- Jenkinson, R. H., Wendahl, A., Zhang, Y. & Sindt, J. E. Migration of epidural leads during spinal cord stimulator trials. *J. Pain Res.* **15**, 2999–3005. <https://doi.org/10.2147/JPR.S378937> (2022).
- Losada-Díaz, F. et al. Differential efficacy of weight loss interventions in patients with versus without diabetes. *Diabetes Ther.* **15**, 2279–2291. <https://doi.org/10.1007/s13300-024-01646-y> (2024).
- Dombovy-Johnson, M. L., D'Souza, R. S., Ha, C. T. & Hagedorn, J. M. Incidence and risk factors for spinal cord stimulator lead migration with or without loss of efficacy: a retrospective review of 91 consecutive thoracic lead implants. *Neuromodulation* **25**, 731–737. <https://doi.org/10.1111/ner.13487> (2022).
- West, T. et al. Incidence of lead migration with loss of efficacy or paresthesia coverage after spinal cord stimulator implantation: systematic review and proportional meta-analysis of prospective studies and randomized clinical trials. *Neuromodulation* **26**, 917–927. <https://doi.org/10.1016/j.neurom.2023.03.016> (2023).
- Bradley, K. The technology: The anatomy of a spinal cord and nerve root stimulator: The lead and the power source. *Pain Med.* **7**, 27–34 (2006).
- Ross, E. & Abejón, D. Improving patient experience with spinal cord stimulation: implications of position-related changes in neurostimulation. *Neuromodulation* **17**(Suppl 1), 36–41. <https://doi.org/10.1111/j.1525-1403.2011.00407.x> (2014).
- Schultz, D. M. et al. Sensor-driven position-adaptive spinal cord stimulation for chronic pain. *Pain Phys.* **15**, 1–12 (2012).
- Parker, J. L., Karantonis, D. M., Single, P. S., Obradovic, M. & Cousins, M. J. Compound action potentials recorded in the human spinal cord during neurostimulation for pain relief. *Pain* **153**, 593–601. <https://doi.org/10.1016/j.pain.2011.11.023> (2012).
- Parker, J. L. et al. Electrically evoked compound action potentials recorded from the sheep spinal cord. *Neuromodulation* **16**, 295–303. <https://doi.org/10.1111/ner.12053> (2013) (discussion 303).
- Ertekin, C. Studies on the human evoked electrospinogram. I. The origin of the segmental evoked potentials. *Acta Neurol. Scand.* **53**, 3–20. <https://doi.org/10.1111/j.1600-0404.1976.tb04321.x> (1976).
- Ertekin, C. Studies on the human evoked electrospinogram. II. The conduction velocity along the dorsal funiculus. *Acta Neurol. Scand.* **53**, 21–38. <https://doi.org/10.1111/j.1600-0404.1976.tb04322.x> (1976).
- Maruyama, Y., Shimoji, K., Shimizu, H., Kuribayashi, H. & Fujioka, H. Human spinal cord potentials evoked by different sources of stimulation and conduction velocities along the cord. *J. Neurophysiol.* **48**, 1098–1107. <https://doi.org/10.1152/jn.1982.48.5.1098> (1982).
- Mekhail, N. et al. Long-term safety and efficacy of close-loop spinal cord stimulation to treat chronic back and leg pain (Evoke): a double-blind, randomised, controlled trial. *Lancet Neurol.* **19**, 123–134. [https://doi.org/10.1016/s1474-4422\(19\)30414-4](https://doi.org/10.1016/s1474-4422(19)30414-4) (2020).
- Russo, M. et al. Effective relief of pain and associated symptoms with close-loop spinal cord stimulation system: preliminary results of the Avalon study. *Neuromodulation* **21**, 38–47. <https://doi.org/10.1111/ner.12684> (2018).
- Russo, M. et al. Sustained long-term outcomes with close-loop spinal cord stimulation: 12-month results of the prospective, multicentre, open-label Avalon study. *Neurosurgery* **87**, E485–e495. <https://doi.org/10.1093/neuros/nyaa003> (2020).
- Mekhail, N. et al. Durability of clinical and quality-of-life outcomes of close-loop spinal cord stimulation for chronic back and leg pain: a secondary analysis of the evoke randomized clinical trial. *JAMA Neurol.* **79**, 251–260. <https://doi.org/10.1001/jamaneuro.2021.4998> (2022).
- Mekhail, N. A. et al. ECAP-controlled close-loop versus open-loop SCS for the treatment of chronic pain: 36-month results of the EVOKE blinded randomized clinical trial. *Reg. Anesth. Pain Med.* **49**, 346–354. <https://doi.org/10.1136/rapm-2023-104751> (2024).
- Rowald, A. et al. Activity-dependent spinal cord neuromodulation rapidly restores trunk and leg motor functions after complete paralysis. *Nat. Med.* **28**, 260. <https://doi.org/10.1038/s41591-021-01663-5> (2022).
- Lorach, H. et al. Walking naturally after spinal cord injury using a brain-spine interface. *Nature* **618**, 126. <https://doi.org/10.1038/s41586-023-06094-5> (2023).
- Capogrosso, M. et al. A brain-spine interface alleviating gait deficits after spinal cord injury in primates. *Nature* **539**, 284. <https://doi.org/10.1038/nature20118> (2016).
- Parker, J. L. et al. Evoked compound action potentials reveal spinal cord dorsal column neuroanatomy. *Neuromodulation* **23**, 82–95. <https://doi.org/10.1111/ner.12968> (2020).
- Calvert, J. S. et al. Spatiotemporal distribution of electrically evoked spinal compound action potentials during spinal cord stimulation. *Neuromodulation* **26**, 961–974. <https://doi.org/10.1016/j.neurom.2022.03.007> (2023).
- Dietz, B. E., Mugan, D., Vuong, Q. C. & Obara, I. Electrically evoked compound action potentials in spinal cord stimulation: implications for preclinical research models. *Neuromodulation* **25**, 64–74. <https://doi.org/10.1111/ner.13480> (2022).
- Versantvoort, E. M. et al. Evoked compound action potential (ECAP)-controlled close-loop spinal cord stimulation in an experimental model of neuropathic pain in rats. *Bioelectron. Med.* **10**, 2. <https://doi.org/10.1186/s42234-023-00134-1> (2024).
- Sharma, M. et al. Novel evoked synaptic activity potentials (ESAPs) elicited by spinal cord stimulation. *eNeuro* <https://doi.org/10.1523/eneuro.0429-22.2023> (2023).
- Deshmukh, A. et al. Epidural Spinal Cord Recordings (ESRs): sources of neural-appearing artifact in stimulation evoked compound action potentials. *J. Neural Eng.* <https://doi.org/10.1088/1741-2552/ad7f8b> (2024).
- Ali, R. & Schwab, J. M. History and future of spinal cord stimulation. *Neurosurgery* **94**, 20–28. <https://doi.org/10.1227/neu.00000000002654> (2024).



33. Miller, J. P. et al. Parameters of spinal cord stimulation and their role in electrical charge delivery: a review. *Neuromodulation* **19**, 373–384. <https://doi.org/10.1111/ner.12438> (2016).

### Acknowledgements

This work was supported by Beijing Science and Technology Plan Project Z241100007724002, and the National Natural Science Foundation of China, 51977205, 52077209. We thank New Cloud Medical, Inc., China, for providing the epidural lead. Neither of the mentioned funders or company was involved in the conception and performance of the study.

### Author contributions

N. W.: research design; data collection and analysis; manuscript writing, reviewing and editing. Z. W.: data collection and analysis; manuscript reviewing and editing. C. Z.: research design; supervision. C. W.: funding acquisition; supervision. X. H.: funding acquisition; supervision. J. B.: research design; supervision. G. Z.: research design; data analysis; manuscript reviewing and editing; funding acquisition; supervision. All authors read and approved the final version of the manuscript for submission.

### Declarations

#### Competing interests

The authors declare no competing interests.

#### Additional information

**Correspondence** and requests for materials should be addressed to G.Z.

**Reprints and permissions information** is available at [www.nature.com/reprints](http://www.nature.com/reprints).

**Publisher's note** Springer Nature remains neutral with regard to jurisdictional claims in published maps and institutional affiliations.

**Open Access** This article is licensed under a Creative Commons Attribution-NonCommercial-NoDerivatives 4.0 International License, which permits any non-commercial use, sharing, distribution and reproduction in any medium or format, as long as you give appropriate credit to the original author(s) and the source, provide a link to the Creative Commons licence, and indicate if you modified the licensed material. You do not have permission under this licence to share adapted material derived from this article or parts of it. The images or other third party material in this article are included in the article's Creative Commons licence, unless indicated otherwise in a credit line to the material. If material is not included in the article's Creative Commons licence and your intended use is not permitted by statutory regulation or exceeds the permitted use, you will need to obtain permission directly from the copyright holder. To view a copy of this licence, visit <http://creativecommons.org/licenses/by-nc-nd/4.0/>.

© The Author(s) 2024